

Effect of electron-hole separation on optical properties of individual Cd(Se,Te) Quantum Dots

M. Ściesiek,¹ J. Suffczyński,^{1,*} W. Pacuski,¹ M. Parlińska-Wojtan,² T. Smoleński,¹ P. Kossacki,¹ and A. Golnik¹

¹*Institute of Experimental Physics, Faculty of Physics, University of Warsaw, Pasteura 5 St., 02-093 Warsaw, Poland*

²*Institute of Nuclear Physics, Polish Academy of Sciences, Radzikowskiego 152 St., 31-342 Kraków, Poland*

(Dated: March 2, 2016)

Cd(Se,Te) Quantum Dots (QD) in ZnSe barrier typically exhibit a very high spectral density, which precludes investigation of single dot photoluminescence. We design, grow and study individual Cd(Se,Te)/ZnSe QDs of low spectral density of emission lines achieved by implementation of a Mn-assisted epitaxial growth. We find an unusually large variation of exciton-biexciton energy difference ($3 \text{ meV} \leq \Delta E_{X-XX} \leq 26 \text{ meV}$) and of exciton radiative recombination rate in the statistics of QDs. We observe a strong correlation between the exciton-biexciton energy difference, exciton recombination rate, splitting between dark and bright exciton, and additionally the exciton fine structure splitting δ_1 and Landé factor. Above results indicate that values of the δ_1 and of the Landé factor in the studied QDs are dictated primarily by the electron and hole respective spatial shift and wavefunctions overlap, which vary from dot to dot due to a different degree of localization of electrons and holes in, respectively, CdSe and CdTe rich QD regions.

PACS numbers: 78.55.Et, 78.55.-m, 78.67.Hc, 71.35.Ji

I. INTRODUCTION

Three dimensional quantum confinement of electrons (e) and holes (h), such as in a semiconductor Quantum Dot (QD) potential, results in a variety of effects resulting from a discrete energy levels structure and an increased overlap between the e and h . Typically, a QD and a surrounding barrier are made of materials sharing a common cation, to recall example of InAs/GaAs, CdTe/ZnTe or CdSe/ZnSe QDs. The QDs for which the QD and the barrier materials have no common atom are by far less investigated, despite of several advantages they offer. In the case of such QDs with type-I confinement one should mention here larger band offsets providing higher confining potentials for both, e and h . Such mixed structures may lead also to type-II confinement, with a decreased wavefunction overlap of the confined e and h . Such increased e - h spatial separation and resulting enhancement of confined carriers lifetimes is highly attractive for studies of magnetic polaron in semimagnetic QDs^{1,2} or Aharonov-Bohm effect,³ as well as for implementation of QDs in photovoltaic devices⁴⁻⁶. The intermediate case between type-I and type-II confinement, as in the present study, offers a chance of investigation of the impact of e and h wavefunctions overlap on properties of excitonic QDs emission.

In the present work, we design, produce and study individual Cd(Se,Te) QDs embedded in ZnSe barrier. Any composition gradient within the Cd(Se,Te) QD volume results in a decreased spatial overlap of wavefunctions of the e and h , due to localization of the e and h in regions, which are richer, respectively, in CdTe and CdSe (see Figure 1 providing a scheme of respective band alignments).

We implement a Mn-assisted epitaxial growth, which allows us to obtain a very low spectral density of the QDs, which enables us to study emission of single QDs. We find a wide distribution of exciton (X) and biexciton

(XX) emission energy difference ($3 \text{ meV} \leq \Delta E_{X-XX} \leq 26 \text{ meV}$). A large scatter is found also for the X lifetime (280 - 620 ps). A statistics collected on several QDs indicates that the ΔE_{X-XX} is strongly correlated with the X lifetime and a bright-dark exciton splitting δ_0 , both quantities being a direct measure of e - h wavefunctions overlap.⁷⁻⁹ In addition, we establish that the ΔE_{X-XX} is strongly correlated with such QD emission properties as the magnitude of the X fine structure exchange splitting δ_1 and Landé-factor. This indicates a way for a straightforward identification of QDs with properties desired for a given implementation^{10,11} without a need of in-depth studies, like emission dynamics or magnetophotoluminescence. The reported distinct dependence of the X fine structure splittings and Landé factor on a degree of e - h wavefunction overlap has been rarely observed in II-VI QD systems so far, despite that it was well established in the case of III-V low dimensional heterostructures¹²⁻¹⁵. Here, we benefit from the fact that, in contrary to the case of typical binary II-VI QD systems, the e - h separation changes significantly from QD to QD, enabling us to perform a systematic study.

II. EXPERIMENT

For micro-Photoluminescence (μ -PL) studies the sample is placed in a pumped helium cryostat (temperature down to $T = 1.5 \text{ K}$) equipped with a superconducting split coil magnet. A magnetic field of up to $B = 10 \text{ T}$ is applied either in Faraday ($\vec{k} \parallel \vec{B}$) or Voigt ($\vec{k} \perp \vec{B}$) configuration. The magnetic field is perpendicular or parallel to the sample surface in this two respective cases. The QDs emission is excited above the barrier bandgap either in a continuous-wave mode at $E_{exc} = 3.06 \text{ eV}$ ($\lambda_{exc} = 405 \text{ nm}$) or in a pulsed mode (100 fs pulse duration, 75 MHz repetition rate) at 3.26 eV ($\lambda_{exc} = 380 \text{ nm}$). The

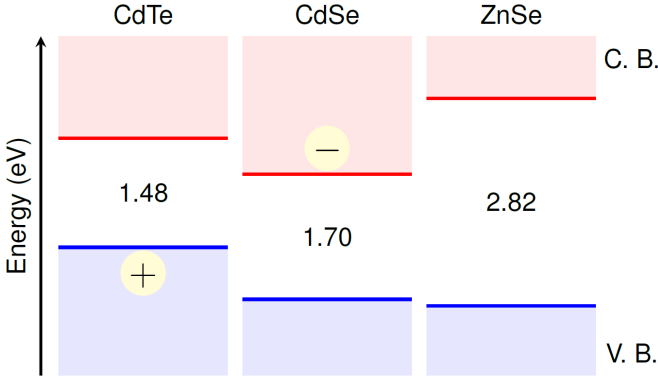


FIG. 1: Band gap energies and relative band offsets for CdTe, CdSe and ZnSe.^{16,17}

excitation beam is focused on the sample surface down to $0.5 \mu\text{m}$ diameter spot with an immersion type microscope objective¹⁸ ($\text{NA} = 0.72$). In the time-integrated measurement the signal is detected using a CCD camera coupled to a 0.75 m spectrometer ($50 \mu\text{eV}$ of overall spectral resolution). Linear and circular polarizations of the signal are resolved. In the time-resolved $\mu\text{-PL}$ measurements, the signal is detected by a Hamamatsu Photonics C5680 streak camera with 5 ps temporal resolution.

The scanning transmission electron microscope (STEM) micrographs of the samples are obtained in high-angle annular dark field detector using FEI Tecnai Osiris instrument. The analysis is carried out at an acceleration voltage of 200 keV and point resolution of $\sim 1.36 \text{ \AA}$. In order to determine the concentration of Zn, Se, Te and Cd in the structure cross-section, a local chemical analysis by energy-dispersive X-ray spectroscopy (EDX) is performed on the 100 nm thick specimen. The TEM specimen is prepared using the classical method of mechanical polishing followed by ion milling down to electron transparency.

III. CD(SE,TE)/ZNSE QUANTUM DOTS PRODUCED BY A MN-ASSISTED EPITAXIAL GROWTH

So far, mixed, Se and Te based, QDs were achieved primarily by a colloidal synthesis^{19–25}. However, integration of such colloidal QDs into operational devices might be challenging. It should be easier in the case of epitaxially grown structures, which offer also a feasibility of p- and n- type doping. On the other hand, strain resulting from a very large lattice mismatch^{26–30} between CdTe ($a_{\text{CdTe}} = 0.648 \text{ nm}$) and ZnSe ($a_{\text{ZnSe}} = 0.567 \text{ nm}$) (above 14%) leads to a high spatial density of QDs combining these two compounds. This has precluded spectroscopy of individual QDs in such mixed type systems so far.^{2,3,29–34}

Cd(Se,Te)/ZnSe QDs presented in this letter are grown by molecular beam epitaxy on a $1 \mu\text{m}$ thick ZnSe buffer deposited on a GaAs substrate. They form in a self-

assembled mode out of atomic layers of Se, Cd, Te, Cd, and Se (each one for time of 15 sec) consecutively deposited at temperature of the substrate set to $335 \text{ }^\circ\text{C}$. An approximately monolayer thick CdSe layer ($a_{\text{CdSe}} = 0.608 \text{ nm}$) inserted between CdTe layer and ZnSe diminishes the strain resulting from the CdTe and the ZnSe lattice mismatch.^{29,30} A small flux of the Mn ions assists deposition of the Te layer. The QD layer is covered with a 80 nm thick ZnSe cap. A reference sample, for which no Mn ions are introduced is also grown under the same conditions.

The presence of Mn induces a significant decrease of spectral density of QD emission lines (see Fig. 2). A spatial density of emitting QDs estimated from $\mu\text{-PL}$ spectra drops from $2000/\mu\text{m}^2$ in the case of the reference sample down to $100/\mu\text{m}^2$ in the case of the sample produced by the Mn-assisted growth. The reduction of QD density for over an order of magnitude results most likely from a reduced mobility of adatoms on the sample surface during the QD nucleation when the Mn atoms are present.³⁵ The energy of QDs emission lowered with respect to the reference sample case (Fig. 2) suggests that the presence of Mn induces also an increased QD size. A qualitatively similar, strong effect of Mn incorporation on the surface morphology and plastic relaxation has been recently reported on also for (Al,Ga)N/GaN heterostructures.³⁶

The HAADF micrographs confirm the presence of a QD layer in the studied structures (see Fig. 3a)). Chemical analysis involving the EDX spectroscopy reveals an expected decrease of the signal related to Zn (Fig. 3b) and an increase of the signal related to Cd (Fig. 3c)) in the QD layer. Not complete vanishing of the signal related to the Zn in the QD layer (Fig. 3b)) is understood when taking into account that the specimen thickness (100 nm) is larger than an individual QD diameter. In such a case signals from both, the Cd(Se,Te) QDs and the ZnSe barrier, contribute to the EDX spectra in the QD layer spatial region.

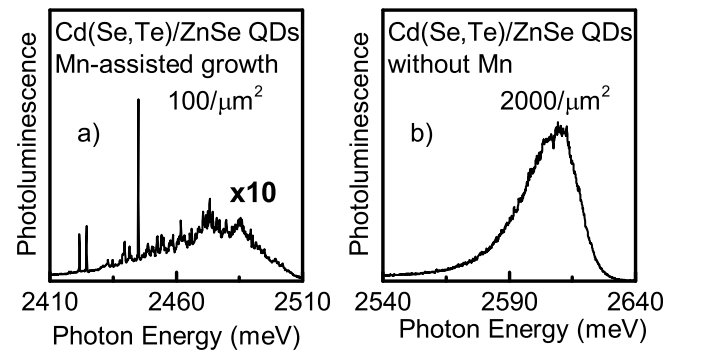


FIG. 2: $\mu\text{-Photoluminescence}$ spectra of: a) Cd(Se,Te)/ZnSe QDs produced by Mn-assisted growth (note that the signal intensity is multiplied by 10), b) reference Cd(Se,Te)/ZnSe QDs. Much decreased spectral density of QD emission lines is evidenced in a). The estimated QDs spatial densities are provided in each panel.

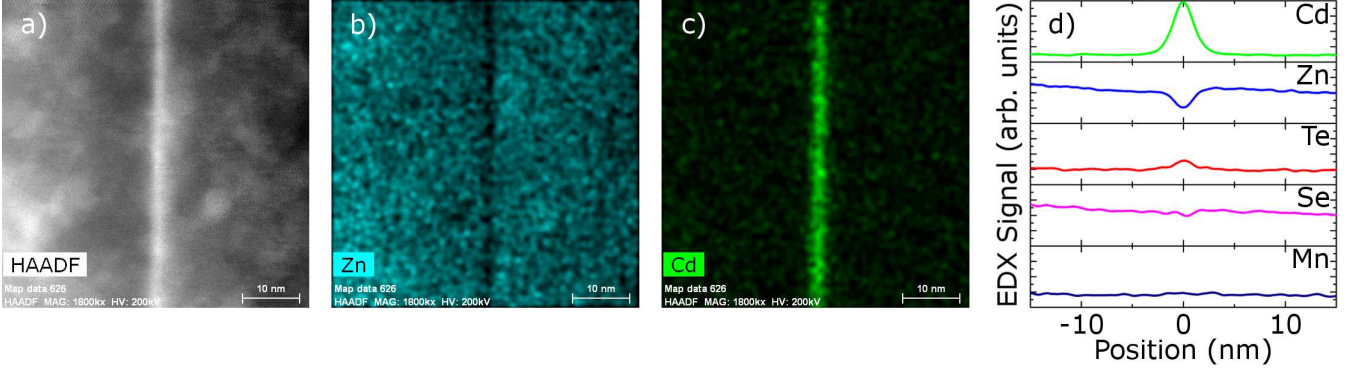


FIG. 3: a) Scanning transmission electron microscope image with the clearly visible layer of Cd(Se,Te)/ZnSe QDs. EDX maps revealing an increase of Cd content (b) and a decrease of Zn content (c) in the QD layer. d) Vertically integrated EDX signal vs the distance from the QDs plane for Cd, Zn, Te, Se and Mn.

Figure 3d) shows the vertically integrated EDX signal for Zn, Se, Cd, Te, Mn as a function of the distance from the QDs plane. It confirms in a direct way the intended presence of the Se and Te atoms in the QDs layer. The average tellurium content in the QDs is determined to $x_{\text{Te}} = 0.22 \pm 0.03$ using a procedure described in the Appendix. Note that the Mn concentration is too low to be detected by the chemical analysis.

IV. RESULTS

A. Impact of e - h wavefunctions overlap on confined exciton dynamics and isotropic part of e - h exchange interaction

A temporal evolution of the emission spectrum of a selected Cd(Se,Te)/ZnSe QD following the excitation pulse is presented in an image acquired by the streak camera (Fig. 4a)). Excitonic transitions shown are identified as the recombination of the X and XX confined in the same QD.³⁷ A doublet of lines evidenced in the case of both, the X and XX, reflects a fine structure exchange splitting δ_1 characteristic for a neutral exciton confined in an anisotropic QD.^{9,38}

Emission lifetime at the energy of the X and XX transitions is determined by fitting of a monoexponential decay curve to the emission intensity at respective cross-sections of the streak camera image (see Fig. 4a)). The X lifetime determined for the selected QD equals to 450 ps. In the QD statistics, the X lifetime ranges from 620 ps, which is rather long for II-VI epitaxial QDs, down to 280 ps, in consistency with the previous reports on CdSe/ZnSe QDs.³⁹ The resulting decay rates Γ_X determined as an inverse of the lifetime are plotted against the X-XX energy difference ΔE_{X-XX} in Fig. 4b). It is seen that the Γ_X significantly increases with the increasing ΔE_{X-XX} . We note that the biexciton decay time of 120 ps corresponds to the decay rate (Γ_{XX}) around 9 ns^{-1} , that is up to 6 times faster than

the Γ_X , much more than observed previously for the pure CdSe/ZnSe QDs.^{39,40} The Γ_{XX} only slightly increases with the ΔE_{X-XX} (not shown).

In order to assess factors governing the X lifetime, we determine the bright-dark exciton splitting δ_0 resulting from isotropic component of the e - h exchange interaction. The δ_0 has been shown to be a direct measure of the e - h wavefunctions overlap.^{8,9,41} To determine the δ_0 we brighten the dark exciton state X_d by application of the magnetic field in a direction parallel to the sample plane (see the inset to Fig. 4c)).⁴² We trace the energy position of the X_d as a function of the magnetic field and we determine its energy in the limit of zero magnetic field by extrapolation. Values of the δ_0 of the order of 1 meV are found, as expected for II-VI QDs.^{38,39,43} We find that the δ_0 increases with the increasing ΔE_{X-XX} (see Fig. 4c)). Comparison of Figs. 4b) and c) reveals a high degree of correlation between the exciton radiative decay rate and the δ_0 . This confirms that: (i) dominating contribution to the δ_0 comes from a short-range component of the e - h exchange interaction within the exciton, in agreement with previous theoretical considerations,^{8,9,41,42} (ii) the X decay in the studied QDs is governed by a radiative recombination, while non-radiative processes are negligible.

A large range of variation of the ΔE_{X-XX} , Γ_X and δ_0 suggests that the e - h spatial separation changes strongly from dot to dot. The increase of the exciton radiative decay rate and of the δ_0 with the increasing ΔE_{X-XX} allows us to treat the ΔE_{X-XX} as an estimate of the degree of e - h wavefunctions overlap in the further discussion. Time integrated measurements presented in Sec. IV B shed more light on optical properties of the studied QDs.

B. Impact of e - h wavefunctions overlap on Landé factor and anisotropic part of e - h exchange interaction

The Figure 5 shows example emission spectra of two individual QDs (labeled as QD1 and QD2), both

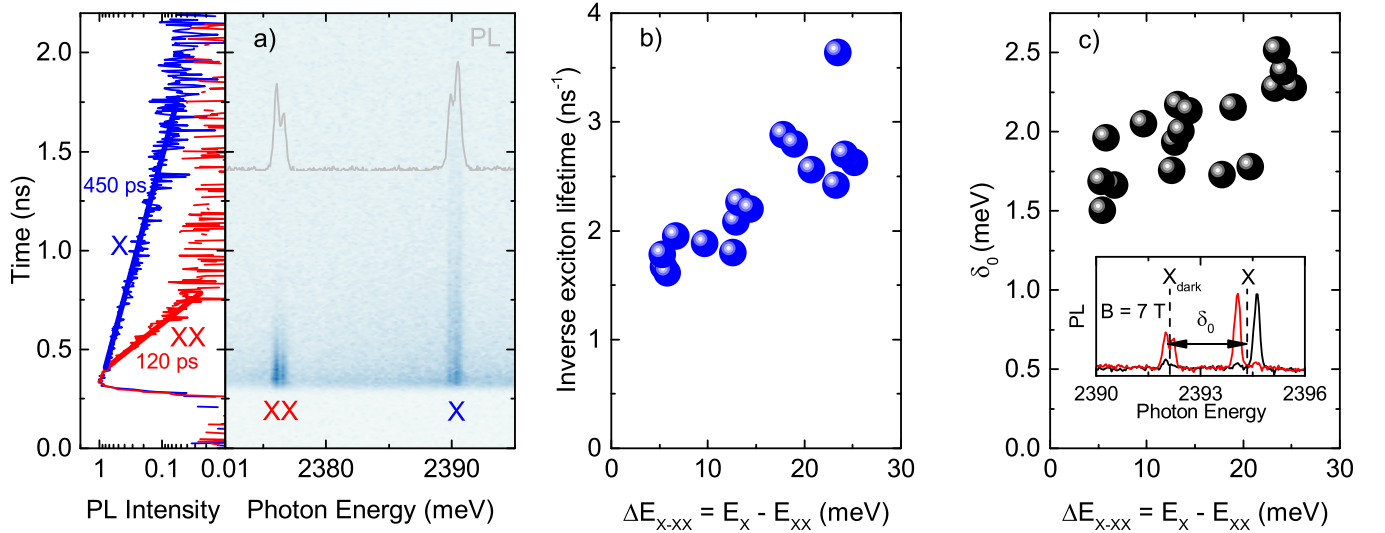


FIG. 4: a) Streak camera image with the emission intensity profile as a function of time (left panel) and of energy for a single Cd(Se,Te)/ZnSe QD. b) Decay rate of the X as a function of energy difference ΔE_{X-XX} between the X and the XX. c) Splitting δ_0 between bright and dark exciton transitions as a function of the ΔE_{X-XX} . Inset: The bright and dark (X_d) exciton transitions of an example QD in magnetic field applied parallel to the sample plane resolved in orthogonal linear polarizations.

coming from the sample produced by the Mn-assisted growth. The emission lines are identified as the X and XX recombination.³⁷ The energy difference ΔE_{X-XX} amounts to 2.99 meV and 20.38 meV in the case of the QD1 and the QD2, respectively. As discussed in the previous Section, the ΔE_{X-XX} acts as a measure of the e - h wavefunction overlap. Thus, the QD1 and QD2 represent two extreme cases of a "small" and "large" e - h overlap, respectively. Note that the QD1 exhibits much lower intensity as compared to the QD2, as expected for a QD with a decreased exciton oscillator strength resulting from a decreased e - h overlap.^{42,44}

The spectra of the XX and X transitions from the QD1 and the QD2 plotted as a function of a detected linear polarization angle reveal two linearly polarized orthogonal components (see panels c-f) in the Fig. 5). An exact antiphase of two components of the X doublet with respect to the XX doublet confirms that the transitions indeed originate from the same QD.³⁷ The fine structure splitting δ_1 for the X and XX from the QD1 amounts to 0.61 meV. In the case of the QD2, much smaller δ_1 equal to 0.07 meV is found.

Figures. 5g) and h) show evolution of the X transition in the magnetic field applied in the Faraday configuration. The black lines represent the simulation of a Zeeman splitting of the exciton ground state in an anisotropic QD following the equation $E_X(B) = E_0 \pm \frac{1}{2} \sqrt{\delta_1^2 + (g\mu_B B)^2}$, where E_0 represent transition energy at $B = 0$ T, δ_1 is the X fine-structure splitting, while g and μ_B represent parallel excitonic Landé factor and Bohr magneton, respectively. The g -factor determined from the fit equals to 1.61 for the QD2, which is quite typical value for CdSe/ZnSe QDs. In contrast, the $g = 0.95$

found for the QD1 is atypically small as for the QD based on any selenium or tellurium compound. The parameters describing the X emission determined in this Subsection for the QD1 and QD2 suggest that in the studied QDs the δ_1 decreases, while the g increases with the increasing ΔE_{X-XX} . The results obtained on a statistics of around twenty QDs are discussed in the next Subsection.

C. Discussion

The values of the excitonic Landé factor and the δ_1 determined for a number of Cd(Se,Te)/ZnSe QDs are plotted against the ΔE_{X-XX} in Fig. 6a). The values for typical, binary type CdTe/ZnTe and CdSe/ZnSe QDs are also presented for a reference (after Ref. 45).

A striking property of the studied QDs is that the ΔE_{X-XX} covers a very wide energy range from 3 meV to 25 meV (see Fig. 4 and Fig. 6). In the case of CdSe or CdTe based QDs the ΔE_{X-XX} exhibits typically a low scatter and remains in a relatively narrow range of 20-25 meV^{38-40,43,45-48} or 12-15 meV^{44-46,49,50}, respectively. Hence, the ΔE_{X-XX} in our case spans from values typical for the CdSe/ZnSe QDs, through values typical for the CdTe/ZnTe QDs, down to much lower values, which were not observed before for the CdSe or the CdTe based QDs systems and which would not be expected for the Cd(Se,Te)/ZnSe QDs if they were homogeneous in a volume. The strongly reduced values of the ΔE_{X-XX} mean that the e and h wavefunctions are separated in space much more than in pure CdSe or CdTe based QDs. It results most likely from a localization of the electrons in CdSe and the holes in CdTe rich regions (see Fig. 1) present in the QD volume. We link the presence of such

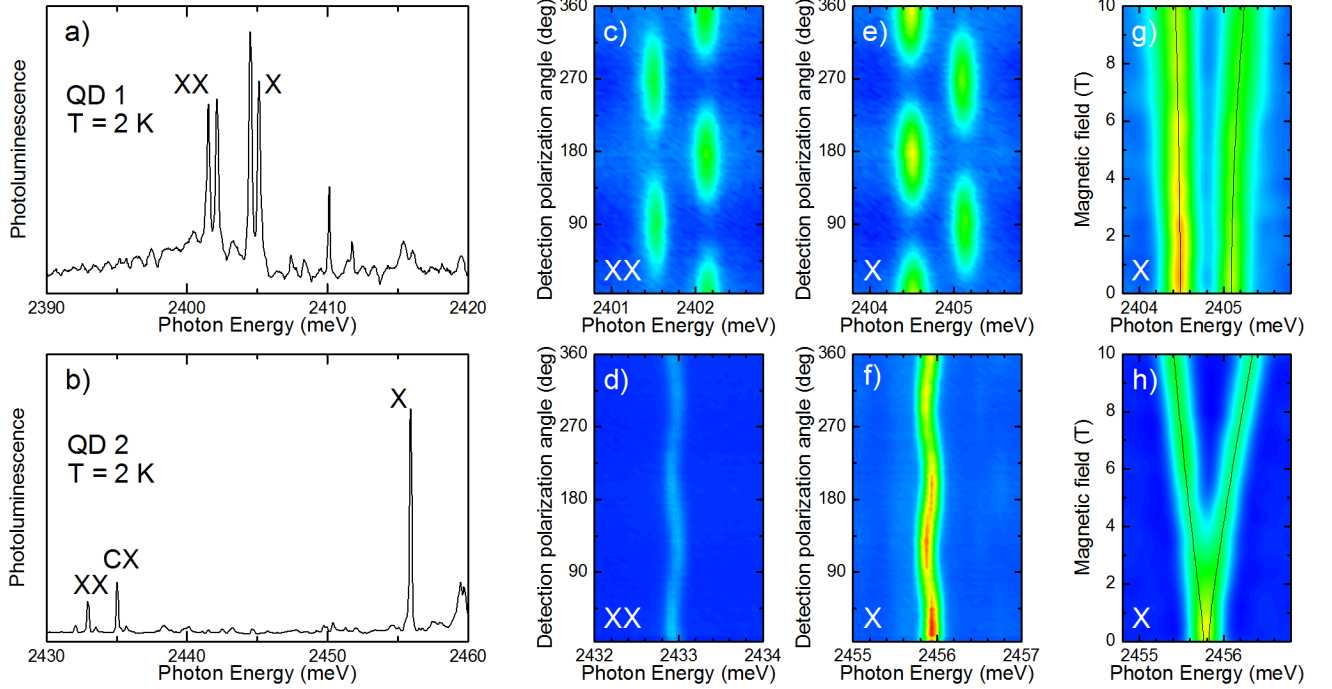


FIG. 5: Exemplary single Cd(Se,Te)/ZnSe QDs from the sample produced by the Mn-assisted growth: a) and b) polarization integrated emission spectra with indicated X, XX and charged exciton (CX) transitions, c) and d) emission spectra *vs* detected linear polarization angle for the XX, e) and f) emission spectra *vs* detected linear polarization angle for the X, g) and h) energy dependence of the X transition on magnetic field applied in Faraday configuration, for QD1 and QD2, respectively. Simulation (black lines) fitted to the experimental data (see text) yields g-factors: $g = 0.95$ and $g = 1.6$ for the QD1 and the QD2, respectively.

regions to the QD layer growth procedure (Sec. III), namely the formation of the QDs out of the deposited consecutively CdSe and CdTe layers. A possible strain would widen the CdTe bandgap and narrow the ZnSe bandgap, even further enhancing the carrier localization effects.²¹

Moreover, the Fig. 6 reveals a clear increase of the excitonic Landé factor and a decrease of the δ_1 with the increasing ΔE_{X-XX} . Such dependencies have not been reported for epitaxial II-VI QDs so far. As it is seen in Fig. 6a), the g-factor attains the value as small as 0.95 for the QD characterized by the $\Delta E_{X-XX} = 2.99$ meV. At the first sight it is surprising, since typical g-factors of CdSe and CdTe QDs are both equal or larger than 1.6, what would result in the g-factor value exceeding 1.6 for a QD made of fully mixed (Cd,Se)Te. This is apparently not the case, which gives a hint that the decreased ΔE_{X-XX} indeed reflects the increased *e-h* separation resulting from a presence of CdTe and CdSe rich regions in the studied QDs. For the Cd(Se,Te)/ZnSe QDs with large values of the ΔE_{X-XX} , the excitonic g-factor is approximately the same as for the pure CdSe/ZnSe QDs (see Fig. 6a)), that is around 1.6.^{38,43} The increase of the parallel Landé factor with the decreasing size of the confining potential in the growth direction, was previously observed in the case

of QWs^{51,52} and arsenide based QDs^{13,14,53,54}, as well as colloidal PbS nanocrystals.⁵⁵ The effect was attributed to a quenching of the orbital momentum of a heavy hole when the hole wavefunction undergoes squeezing in the direction parallel to the magnetic field.⁵⁴

The δ_1 varies with the increasing ΔE_{X-XX} from around 1 meV, the value larger than for reference CdSe/ZnSe or CdTe/ZnTe QDs, down to the values below 0.06 meV (see Fig. 6b)). It has been shown previously that a dominant contribution to the δ_1 comes from the long-range component of the *e-h* exchange interaction.^{7-9,41} The magnitude of the δ_1 , similarly as the magnitude of the short-range component, have been shown to increase with a decreasing QD size (thus with the increasing *e-h* overlap).^{7-9,41} Thus, in the presently studied QDs, one should expect enhancement of the δ_1 with the ΔE_{X-XX} . This is, however, not the case, what indicates that in the studied QDs, not just the overall *e* and *h* wavefunctions overlap, but specifically the anisotropy of the exciton wavefunction in the QD plane provides a main contribution to the δ_1 . A decrease of δ_1 with a decreasing QD size was previously observed in the case of epitaxially grown InAs/GaAs QDs^{12,56} and attributed to the dominating influence of piezoelectricity or heavy hole-light hole subbands mixing effects. In our case, the increase of the

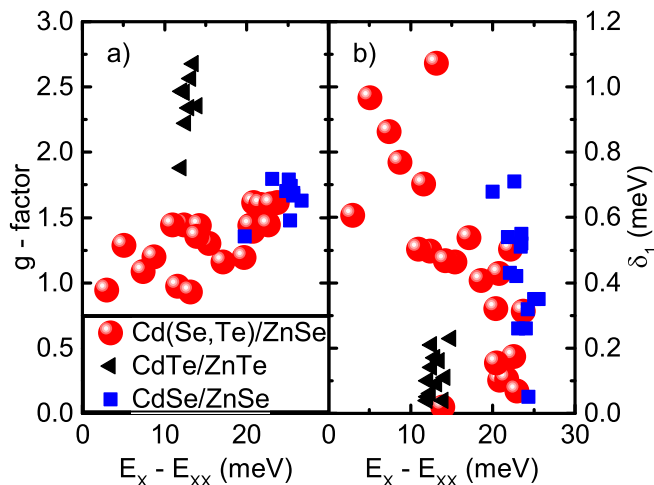


FIG. 6: Exciton parameters describing Cd(Se,Te)/ZnSe QDs produced by the Mn-assisted growth: a) Landé factor and b) fine-structure splitting δ_1 , plotted as a function of exciton - biexciton energy difference ΔE_{X-XX} . Respective values for CdSe/ZnSe and CdTe/ZnTe QDs are also shown for a reference (after Ref. 45).

δ_1 is correlated rather with the increasing Te content in the Cd(Se,Te)/ZnSe QDs, which translates into a larger respective spatial shift of the e and h in the QD plane.

We note that for the Cd(Se,Te)/ZnSe QDs with large values of the ΔE_{X-XX} not only the g-factor, but also the fine structure splitting δ_1 (0.1 - 0.3 meV) matches the one of the pure CdSe/ZnSe QDs^{38,43} (see Fig. 6b)). This points toward binary type QD composition in the case of these QDs. This results most likely from an efficient substitution of Te atoms by Se atoms during the QD growth, due to a much higher sticking coefficient of the Se atoms as compared to the Te atoms.^{57,58}

No systematic dependence of a diamagnetic coefficient γ on the ΔE_{X-XX} is found (not shown). The γ is typically related to a span of the e and h wavefunctions in the QD plane. Thus, we state the e - h wavefunctions overlap varies from dot to dot mainly in the sample growth direction.

V. CONCLUSIONS

We have investigated systematically the impact of the electron-hole separation on optical properties of individual Cd(Se,Te)/ZnSe quantum dots. The reduced spectral density of QD emission lines obtained thanks to the Mn-assisted epitaxial growth has provided us an access to individual QDs emission. A statistics involving several individual QDs is collected. We have found that there exists a high degree of correlation between quantities being a direct measure of the e - h wavefunctions overlap, such as the exciton radiative decay rate and the bright-dark exciton splitting δ_0 , with the exciton-biexciton energy difference ΔE_{X-XX} . The ΔE_{X-XX} varies significantly

from dot to dot, i.e., it changes from values typical for CdSe/ZnSe QDs and CdTe/ZnTe QDs, down to values as small as 3 meV, which were not reported previously for either of the two binary type systems. We attribute the wide distribution of the ΔE_{X-XX} to a wide range of variation of the studied QDs composition and inhomogeneity affecting the e - h wavefunctions overlap. In particular, the strongly reduced ΔE_{X-XX} points toward a presence of the CdTe and CdSe rich regions in the studied QDs, which localize electron and hole, respectively, and account for an increased e - h separation.

Moreover, in contrary to a simple expectation, the Cd(Se,Te)/ZnSe QDs g-factor is smaller than g-factors found previously in case of both, CdSe/ZnSe QDs and CdTe/ZnTe, binary type QD systems. Additionally, a distinct and so far not observed for II-VI QDs, dependencies of the g-factor and of the fine structure exchange splitting δ_1 on the ΔE_{X-XX} are found. The g-factor increases, while the δ_1 decreases with the increasing ΔE_{X-XX} , that is with the increasing e - h wavefunctions overlap.

Since an ability of selection of QDs with precisely defined emission properties is a prerequisite for QDs practical implementations, the demonstrated parametrization of the g-factor or the δ_1 by the ΔE_{X-XX} in the studied QDs provides a perspective for overcoming of the limits related to a scatter of the g-factor and the δ_1 values observed typically in the QDs ensemble. At the same time, further efforts for obtaining QDs with a degree of separation of confined carriers controlled on the production stage are still desired.

Acknowledgments

This work was supported by the Polish National Research Center projects DEC-2013/10/E/ST3/00215, DEC-2013/09/B/ST3/02603, DEC-2011/02/A/ST3/00131, DEC-2015/18/E/ST3/00559, and DEC-2011/02/A/ST3/00131, by the Polish Ministry of Science and Higher Education in years 2012-2016 as a research grant "Diamantowy Grant" and "Inventus Plus" grant IP2014 034573. One of us (T.S.) was supported by the Foundation for Polish Science through the START programme. The work was carried out with the use of CePT, CeZaMat, and NLTK infrastructures financed by the European Union - the European Regional Development Fund within the Operational Programme "Innovative Economy". The use of the FEI Tecnai Osiris TEM instrument located at the Facility for Electron Microscopy & Sample Preparation of the University of Rzeszów is acknowledged.

Appendix

Determination of the average molar density x of the Te atoms in the Cd(Se,Te) QDs bases on relative changes of

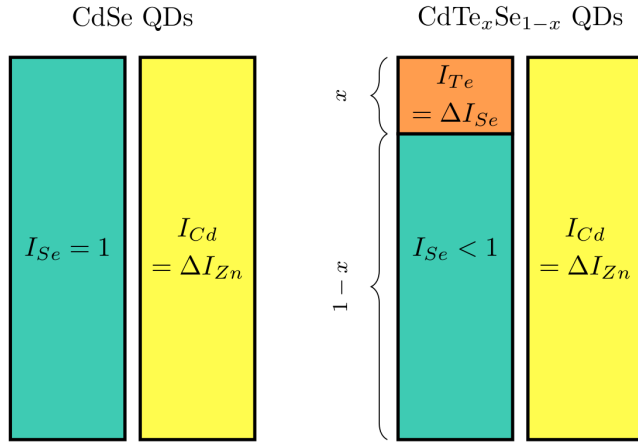


FIG. 7: Determination of average Te content in the Cd(Se,Te) QDs: the ratio of the Te to Cd atom densities, that is the average molar density x of the Te in the Cd(Se,Te) QDs is set by the ratio of a relative decrease ΔI_{Se} of the EDX signal of Se to a relative decrease ΔI_{Zn} of the EDX signal of Zn (which is substituted by Cd).

a vertically integrated EDX signal. Formation of pure CdTe QDs would result in equal relative (with respect to the maximum determined for the barrier layer) decrease

of Zn and Se signal in the QDs layer. As evidenced in Fig. 3d), showing the vertically integrated EDX signal for of Zn, Se, Cd, Te, and Mn as a function of the distance from the QDs plane, this is, however, not the case. The different relative decrease of the Zn and Se signal in the QDs layer confirms the presence of the Se atoms in the QDs. Since a number of the Cd anions in the Cd(Se,Te) QDs is equal to the sum of the, substituting each other, Te and Se cations, the ratio of a relative decrease ΔI_{Se} of the Se signal to a relative decrease ΔI_{Zn} of the Zn signal (substituted by Cd) gives the ratio of the Te to Cd atom densities, thus the average molar density x of the Te atoms in the Cd(Se,Te) QDs:

$$x = \frac{\Delta I_{Se}}{\Delta I_{Zn}}$$

We note that the EDX signal detection sensitivity depends in unknown way on a given element. As a result, the absolute values of EDX signal for each element are also not known. It is known, however, that the signals for Se and Zn in the ZnSe barrier region attain their maximum values. These values serve as a reference in determination of relative changes of the EDX signal in the QD layer for respective elements.

* Electronic address: Jan.Suffczynski@fuw.edu.pl

- ¹ L. Kłopotowski, L. Cywiński, P. Wojnar, V. Voliotis, K. Fronc, T. Kazimierzczuk, A. Golnik, M. Ravaro, R. Grousson, G. Karczewski, and T. Wojtowicz, *Magnetic polaron formation and exciton spin relaxation in single Cd_{1-x}Mn_xTe quantum dots*, Phys. Rev. B **83**, 081306 (2011).
- ² B. Barman, R. Oszwaldowski, L. Schweidenback, A. H. Russ, J. M. Pientka, Y. Tsai, W.-C. Chou, W. C. Fan, J. R. Murphy, A. N. Cartwright, I. R. Sellers, A. G. Petukhov, I. Žutić, B. D. McCombe, and A. Petrou, *Time-resolved magnetophotoluminescence studies of magnetic polaron dynamics in type-II quantum dots*, Phys. Rev. B **92**, 035430 (2015).
- ³ I. R. Sellers, V. R. Whiteside, I. L. Kuskovsky, A. O. Govorov, and B. D. McCombe, *Aharonov-Bohm Excitons at Elevated Temperatures in Type-II ZnTe/ZnSe Quantum Dots*, Phys. Rev. Lett. **100**, 136405 (2008).
- ⁴ S. Boyer-Richard, C. Robert, L. Gérard, J.-P. Richters, R. André, J. Bleuse, H. Mariette, J. Even, and J.-M. Jancu, *Atomistic simulations of the optical absorption of type-II CdSe/ZnTe superlattices*, Nanoscale Research Letters **7**, 543 (2012).
- ⁵ I. Bragar and P. Machnikowski, *Intraband absorption in finite, inhomogeneous quantum dot stacks for intermediate band solar cells: Limitations and optimization*, J. Appl. Phys. **112** (2012).
- ⁶ S. Dhomkar, U. Manna, L. Peng, R. Moug, I. Noyan, M. Tamargo, and I. Kuskovsky, *Feasibility of submonolayer ZnTe/ZnCdSe quantum dots as intermediate band solar cell material system*, Solar Energy Materials and Solar

- Cells **117**, 604 (2013).
- ⁷ A. Franceschetti, L. W. Wang, H. Fu, and A. Zunger, *Short-range versus long-range electron-hole exchange interactions in semiconductor quantum dots*, Phys. Rev. B **58**, R13367 (1998).
- ⁸ T. Takagahara, *Theory of exciton doublet structures and polarization relaxation in single quantum dots*, Phys. Rev. B **62**, 16840 (2000).
- ⁹ M. Bayer, G. Ortner, O. Stern, A. Kuther, A. A. Gorbunov, A. Forchel, P. Hawrylak, S. Fafard, K. Hinzer, T. L. Reinecke, S. N. Walck, J. P. Reithmaier, F. Kloppe, and F. Schäfer, *Fine structure of neutral and charged excitons in self-assembled In(Ga)As/(Al)GaAs quantum dots*, Phys. Rev. B **65**, 195315 (2002).
- ¹⁰ T. Jakubczyk, H. Franke, T. Smoleński, M. Ściesiek, W. Pacuski, A. Golnik, R. Schmidt-Grund, M. Grundmann, C. Kruse, D. Hommel, and P. Kossacki, *Inhibition and Enhancement of the Spontaneous Emission of Quantum Dots in Micropillar Cavities with Radial-Distributed Bragg Reflectors*, ACS Nano **8**, 9970 (2014).
- ¹¹ W. Pacuski, T. Jakubczyk, C. Kruse, J. Kobak, T. Kazimierzczuk, M. Goryca, A. Golnik, P. Kossacki, M. Wiater, P. Wojnar, G. Karczewski, T. Wojtowicz, and D. Hommel, *Micropillar Cavity Containing a CdTe Quantum Dot with a Single Manganese Ion*, Crystal Growth & Design **14**, 988 (2014).
- ¹² R. Seguin, A. Schliwa, S. Rodt, K. Pötschke, U. W. Pohl, and D. Bimberg, *Size-Dependent Fine-Structure Splitting in Self-Organized InAs/GaAs Quantum Dots*, Phys. Rev. Lett. **95**, 257402 (2005).
- ¹³ C. E. Pryor and M. E. Flatté, *Landé g Factors and Orbital*

- Momentum Quenching in Semiconductor Quantum Dots*, Phys. Rev. Lett. **96**, 026804 (2006).
- ¹⁴ N. A. J. M. Kleemans, J. van Bree, M. Bozkurt, P. J. van Veldhoven, P. A. Nouwens, R. Nötzel, A. Y. Silov, P. M. Koenraad, and M. E. Flatté, *Size-dependent exciton g factor in self-assembled InAs/InP quantum dots*, Phys. Rev. B **79**, 045311 (2009).
 - ¹⁵ V. Krápek, P. Klenovský, and T. Šikola, *Excitonic fine structure splitting in type-II quantum dots*, Phys. Rev. B **92**, 195430 (2015).
 - ¹⁶ C. Hsu and J. Faurie, *Summary Abstract: Valence band discontinuities at the heterojunctions between CdTe, ZnTe, and HgTe in the (100) orientation: X-ray photoelectron spectroscopy study*, J. Vac. Sci. Technol. B **6**, 773 (1988).
 - ¹⁷ Y. Hinuma, A. Grüneis, G. Kresse, and F. Oba, *Band alignment of semiconductors from density-functional theory and many-body perturbation theory*, Phys. Rev. B **90**, 155405 (2014).
 - ¹⁸ J. Jasny, J. Sepiol, T. Irngartinger, M. Traber, A. Renn, and U. P. Wild, *Fluorescence microscopy in superfluid helium: Single molecule imaging*, Review of Scientific Instruments **67**, 1425 (1996).
 - ¹⁹ S. Kim, B. Fisher, H.-J. Eisler, and M. Bawendi, *Type-II Quantum Dots: CdTe/CdSe(Core/Shell) and CdSe/ZnTe(Core/Shell) Heterostructures*, Journal of the American Chemical Society **125**, 11466 (2003).
 - ²⁰ R. E. Bailey and S. Nie, *Alloyed Semiconductor Quantum Dots: Tuning the Optical Properties without Changing the Particle Size*, Journal of the American Chemical Society **125**, 7100 (2003).
 - ²¹ A. Smith, A. M. Mohs, and S. Nie, *Tuning the optical and electronic properties of colloidal nanocrystals by lattice strain*, Nat. Nanotechnol. **4**, 56 (2008).
 - ²² D. Dorfs, T. Franzl, R. Osovsky, M. Brumer, E. Lifshitz, T. A. Klar, and A. Eychmüller, *Type-I and Type-II Nanoscale Heterostructures Based on CdTe Nanocrystals: A Comparative Study*, Small **4**, 1148 (2008).
 - ²³ N. Hewa-Kasakarage, N. Gurusinge, and M. Zamkov, *Blue-Shifted Emission in CdTe/ZnSe Heterostructured Nanocrystals*, J. Phys. Chem. C **113**, 4362 (2009).
 - ²⁴ J. He, H. Zhong, and G. D. Scholes, *Electron-Hole Overlap Dictates the Hole Spin Relaxation Rate in Nanocrystal Heterostructures*, Phys. Rev. Lett. **105**, 046601 (2010).
 - ²⁵ L. Li, Y. Chen, Q. Lu, J. Ji, Y. Shen, M. Xu, R. Fei, G. Yang, K. Zhang, J.-R. Zhang, et al., *Electrochemiluminescence energy transfer-promoted ultrasensitive immunoassay using near-infrared-emitting CdSeTe/CdS/ZnS quantum dots and gold nanorods*, Scientific reports **3**, 1529 (2013).
 - ²⁶ M. Konagai, M. Kobayashi, R. Kimura, and K. Takahashi, *ZnSe-ZnTe strained-layer superlattices: A novel material for the future optoelectronic devices*, Journal of Crystal Growth **86**, 290 (1988).
 - ²⁷ B. Gil, T. Cloitre, N. Briot, O. Briot, P. Boring, and R. Aulombard, *Photo-induced screening of the excitonic interaction in ZnSe-ZnTe type-II strained-layer superlattices*, Journal of Crystal Growth **138**, 868 (1994).
 - ²⁸ S. Rubini, B. Bonanni, E. Pelucchi, A. Franciosi, A. Garulli, A. Parisini, Y. Zhuang, G. Bauer, and V. Holý, *ZnSe/CdTe/ZnSe heterostructures*, J. Vac. Sci. Technol. B **18**, 2263 (2000).
 - ²⁹ A. A. Toropov, I. V. Sedova, O. G. Lyublinskaya, S. V. Sorokin, A. A. Sitnikova, S. V. Ivanov, J. P. Bergman, B. Monemar, F. Donatini, and L. Si Dang, *Coexistence of type-I and type-II band lineups in Cd(Te,Se)/ZnSe quantum-dot structures*, Applied Physics Letters **89**, 123110 (2006).
 - ³⁰ I. Sedova, O. Lyublinshaya, S. Sorokin, A. Sitnikova, A. Toropov, F. Donatini, L. S. Dang, and S. Ivanov, *CdSe/ZnSe Quantum Dot Structures Grown by Molecular Beam Epitaxy with a CdTe Submonolayer Stressor*, Semiconductors **41**, 1363 (2007).
 - ³¹ M. Kuo, J. Hsu, J. Shen, K. Chiu, W. Fan, Y. C. Lin, C. H. Chia, W. C. Chou, M. Yasar, R. Mallory, A. Petrou, and H. Luo, *Photoluminescence studies of type-II diluted magnetic semiconductor ZnMnTe/ZnSe quantum dots*, Appl. Phys. Lett. **89**, 263111 (2006).
 - ³² C. Yang, W. J.S., Y. Lai, D. Luo C.W. dna Chen, Y. Shih, S. Jian, and W. Chou, *Formation of a precursor layer in self-assembled CdTe quantum dots grown on ZnSe by molecular beam epitaxy*, Nanotechnology **18**, 385602 (2007).
 - ³³ Y. Gong, W. MacDonald, G. F. Neumark, M. C. Tamargo, and I. L. Kuskovsky, *Optical properties and growth mechanism of multiple type-II ZnTe/ZnSe quantum dots grown by migration-enhanced epitaxy*, Phys. Rev. B **77**, 155314 (2008).
 - ³⁴ W. Fan, S. Huang, W. Chou, M. Tsou, C. Yang, C. Chia, N. D. Phu, and L. H. Hoang, *Growth and optical properties of ZnTe quantum dots on ZnMgSe by molecular beam epitaxy*, Journal of Crystal Growth **425**, 186 (2015).
 - ³⁵ C. Kim, M. Kim, S. Lee, J. Kossut, J. Furdyna, and M. Dobrowolska, *CdSe quantum dots in a $Zn_{1-x}Mn_xSe$ matrix: new effects due to the presence of Mn*, J. Cryst. Growth **214/215**, 395 (2000).
 - ³⁶ T. Devillers, L. Tian, R. Adhikari, G. Capuzzo, and A. Bonanni, *Mn as Surfactant for the Self-Assembling of $Al_xGa_{1-x}N/GaN$ Layered Heterostructures*, Crystal Growth & Design **15**, 587 (2015).
 - ³⁷ A. Kudelski, K. Kowalik, A. Golnik, G. Karczewski, J. Kossut, and J. Gaj, *Spatially correlated 0D exciton states in CdTe/ZnTe semiconductor system*, Journal of Luminescence **112**, 127 (2005).
 - ³⁸ V. D. Kulakovskii, G. Bacher, R. Weigand, T. Kümmell, A. Forchel, E. Borovitskaya, K. Leonardi, and D. Hommel, *Fine Structure of Biexciton Emission in Symmetric and Asymmetric CdSe/ZnSe Single Quantum Dots*, Phys. Rev. Lett. **82**, 1780 (1999).
 - ³⁹ B. Patton, W. Langbein, and U. Woggon, *Trion, biexciton, and exciton dynamics in single self-assembled CdSe quantum dots*, Phys. Rev. B **68**, 125316 (2003).
 - ⁴⁰ G. Bacher, R. Weigand, J. Seufert, V. D. Kulakovskii, N. A. Gippius, A. Forchel, K. Leonardi, and D. Hommel, *Biexciton versus Exciton Lifetime in a Single Semiconductor Quantum Dot*, Phys. Rev. Lett. **83**, 4417 (1999).
 - ⁴¹ T. Takagahara, *Effects of dielectric confinement and electron-hole exchange interaction on excitonic states in semiconductor quantum dots*, Phys. Rev. B **47**, 4569 (1993).
 - ⁴² M. Nirmal, D. J. Norris, M. Kuno, M. G. Bawendi, A. L. Efros, and M. Rosen, *Observation of the "Dark Exciton" in CdSe Quantum Dots*, Phys. Rev. Lett. **75**, 3728 (1995).
 - ⁴³ J. Puls, M. Rabe, H.-J. Wünsche, and F. Henneberger, *Magneto-optical study of the exciton fine structure in self-assembled CdSe quantum dots*, Phys. Rev. B **60**, R16303 (1999).
 - ⁴⁴ P. Sujana, A. J. Peter, and C. W. Lee, *Optical studies of an exciton and a biexciton in a CdTe/ZnTe quantum dot*

- nanostructure*, Optics Communications **336**, 120 (2015).
- ⁴⁵ J. Kobak, T. Smoleński, M. Goryca, J.-G. Rousset, W. Pacuski, A. Bogucki, P. Kossacki, J. Golnik, A. Płachta, P. Wojnar, C. Kruse, D. Hommel, M. Potemski, and T. Kazimierczuk, *Comparison of magneto-optical properties of various excitonic complexes in CdTe and CdSe self-assembled quantum dots*, arXiv:1602.06118.
 - ⁴⁶ J. Kobak, T. Smoleński, M. Goryca, M. Papaż, K. Gietka, A. Bogucki, M. Koperski, J.-G. Rousset, J. Suffczyński, E. Janik, M. Nawrocki, A. Golnik, P. Kossacki, and W. Pacuski, *Designing quantum dots for solotronics*, Nat. Commun. **5**, 3191 (2014).
 - ⁴⁷ J. Piwowar, W. Pacuski, T. Smoleński, M. Goryca, A. Bogucki, A. Golnik, M. Nawrocki, P. Kossacki, and J. Suffczyński, *Epitaxial growth and photoluminescence excitation spectroscopy of CdSe quantum dots in (Zn,Cd)Se barrier*, Journal of Luminescence **173**, 94 (2016).
 - ⁴⁸ T. Smolenski, T. Kazimierczuk, J. Kobak, M. Goryca, A. Golnik, P. Kossacki, and W. Pacuski, *Magnetic Ground State of an Individual Fe^{2+} Ion in Strained Semiconductor Nanostructure*, Nat. Commun. **7**, 10484 (2016).
 - ⁴⁹ L. Besombes, K. Kheng, L. Marsal, and H. Mariette, *Few-particle effects in single CdTe quantum dots*, Phys. Rev. B **65**, 121314 (2002).
 - ⁵⁰ T. Kazimierczuk, T. Smoleński, M. Goryca, L. Kłopotowski, P. Wojnar, K. Fronc, A. Golnik, M. Nawrocki, J. A. Gaj, and P. Kossacki, *Magnetophotoluminescence study of intershell exchange interaction in CdTe/ZnTe quantum dots*, Phys. Rev. B **84**, 165319 (2011).
 - ⁵¹ R. Hannak, M. Oestreich, A. Heberle, and W. Rühle, *Electron g factor in quantum wells determined by spin quantum bits*, Solid State Commun **93**, 313 (1995).
 - ⁵² Q. Zhao, M. Oestreich, and N. Magnea, *Electron and hole g factors in CdTe/CdMgTe quantum wells*, Appl. Phys. Lett. **69**, 3704 (1996).
 - ⁵³ R. Kotlyar, T. L. Reinecke, M. Bayer, and A. Forchel, *Zee-man spin splittings in semiconductor nanostructures*, Phys. Rev. B **63**, 085310 (2001).
 - ⁵⁴ S. J. Prado, C. Trallero-Giner, A. M. Alcalde, V. López-Richard, and G. E. Marques, *Influence of quantum dot shape on the Landé g -factor determination*, Phys. Rev. B **69**, 201310 (2004).
 - ⁵⁵ L. Turyanska, J. H. Blokland, U. Elfurawi, O. Makarovsky, P. C. M. Christianen, and A. Patanè, *Photoluminescence of PbS nanocrystals at high magnetic fields up to 30 T*, Phys. Rev. B **82**, 193302 (2010).
 - ⁵⁶ A. Musiał, P. Podemski, G. Sęk, P. Kaczmarkiewicz, J. Andrzejewski, P. Machnikowski, J. Misiewicz, S. Hein, A. Somers, S. Höfling, et al., *Height-driven linear polarization of the surface emission from quantum dashes*, Semicond. Sci. Technol. **27**, 105022 (2012).
 - ⁵⁷ T. Yao, Y. Makita, and S. Maekawa, *Molecular beam epitaxy of ZnSeTe*, Journal of Crystal Growth **45**, 309 (1978).
 - ⁵⁸ B. Bonef, L. Gérard, J.-L. Rouvière, A. Grenier, P.-H. Jouneau, E. Bellet-Amalric, H. Mariette, R. André, and C. Bougerol, *Atomic arrangement at ZnTe/CdSe interfaces determined by high resolution scanning transmission electron microscopy and atom probe tomography*, Applied Physics Letters **106**, 051904 (2015).